Inorganic Chemistry

Communication

pubs.acs.org/IC

A Single-Chain Magnet with a Very High Blocking Temperature and a Strong Coercive Field

Rafael A. Allão Cassaro,*[,†] Samira G. Reis,[‡] Thamyres S. Araujo,[‡] Paul M. Lahti,[§] Miguel A. Novak,[⊥] and Maria G. F. Vaz*[,‡]

[†]Instituto de Química, Universidade Federal do Rio de Janeiro, 21941-909 Rio de Janeiro, Brazil

[‡]Instituto de Química, Universidade Federal Fluminense, Niterói, 24020-150, Rio de Janeiro, Brazil

[§]Department of Chemistry, University of Massachusetts, Amherst, Massachusetts 01003, United States

[⊥]Instituto de Física, Universidade Federal do Rio de Janeiro, 21941-972, Rio de Janeiro, Brazil

Supporting Information

ABSTRACT: Two isostructural 1D complexes, $[M(hfac)_2NaphNN]_n$ [M = Mn^{II} (**1**) or Co^{II} (**2**); NaphNN = 1-naphthyl nitronylnitroxide], were synthesized and exhibit very strong antiferromagnetic metal−radical exchange coupling. Compound **2** shows slow magnetic relaxation behavior with a high blocking temperature ($T_B \approx 13.2$ K) and a very high coercive field of 49 kOe at 4.0 K.

The motivation to study molecular nanomagnets comes from their potential application in high-density magnetic information storage as well as the challenge of understanding their physical behavior.[1−4] Among this class of compounds, one of the most promising systems is the single-chain magnet (SCM) in which the magnetic behavior arises from large uniaxial-type magnetic anisotropy associated with strong intrachain and negligible interchain magnetic interactions.[5−10] However, so far, few SCMs reported in the literature display high blocking temperatures and high coercivity fields ($T_B > 10$ K; $H_c > 30$ kOe), essential properties for applications.[11,12]

A strategy to make stable SCMs with these characteristics is very appealing, not only to investigate the physical phenomena present in such materials but also to enable the necessary steps for realistic application. Some of us recently reported a substantial change to the common strategy of making metal−radical SCM chains with alkoxyphenyl nitronylnitroxides (NNs), by using NN spin units substituted with a large polycyclic aromatic group to keep the chains structurally isolated.[12,13] The $[Co(hfac)_2PyrNN]_n$ chain, where PyrNN is the radical 2-(1′-pyrenyl)-4,4,5,5-tetramethyl-4,5-dihydro-1*H*-imidazole-3-oxide-1-oxyl, shows a record high blocking temperature of 14 K and a very high coercive field.[12] However, this chain displayed some structural instability, attributed to the loss of solvent entrained in the lattice. Since stability is a crucial point to be considered, as stated before, we sought modification in this strategy to increase the stability while preserving the desired SCM-type behavior and high blocking temperatures.

In this paper, we report two new isostructural magnetic chains, $[M(hfac)_2NaphNN]_n$, where M = Mn^{II} (**1**) or Co^{II} (**2**) and NaphNN is 2-(1′-naphthalenyl)-4,4,5,5-tetramethyl-4,5-dihydro-1*H*-imidazole-3-oxide-1-oxyl. Compound **2** behaves as a SCM with a high blocking temperature and exhibits a very strong coercive field.

The $[M(hfac)_2NaphNN]_n$ chains were made in a single step by reacting $[M(hfac)_2]$ hydrates with NaphNN in a solvent mixture of chloroform and dry *n*-heptane [see the Supporting Information (SI) for details]. These compounds crystallize in the $P2_1/n$ space group, with the metal ion coordinated by four oxygen atoms from two hfac ligands and two oxygen atoms from two cis-coordinated NaphNN radicals (Figure S1). The radical is bridge-coordinated to the metal ions, generating a 2-fold helical chain parallel to the crystallographic *b* axis (Figure 1). The metal(II) ions have

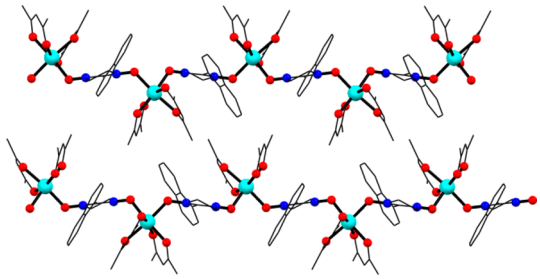

Figure 1. View along the *a* axis of **2**. Methyl groups, hydrogen, and fluorine atoms were omitted for clarity. Atoms: carbon (black), nitrogen (blue), oxygen (red), and cobalt(II) (cyan).

distorted octahedral environments, with M−O bond lengths ranging from 2.088 to 2.178 Å and from 2.039(2) to 2.076(2) Å for **1** and **2**, respectively. The O−M−O bond angles of the cis-coordinated radical oxygen atoms are 85.33(15)° for **1** and 82.47(9)° for **2**. Selected additional bond lengths and angles are given in Table S2. The intrachain distances between metal ions are 7.708(2) Å for **1** and 7.628(2) Å for **2**, while the shortest interchain distances between these ions are 9.721(2) and 9.801(2) Å for **1** and **2**, respectively. The intrachain distances for both compounds are close to those in the $[M(hfac)_2(PyrNN)]_n$ chains,[12,13] but the interchain distances between metal ions are shorter by about 1.3 Å for **1** and **2**, as expected from the smaller size of the naphthyl substituent as well as the absence of lattice solvent molecules. Notably, the

Received: June 25, 2015
Published: September 14, 2015

DOI: 10.1021/acs.inorgchem.5b01431
Inorg. Chem. 2015, 54, 9381−9383

$[Co(hfac)_2(NaphNN)]_n$ chain is stable to ambient conditions (Figure S2).

The χT temperature dependence of **1** (Figure S3) shows the expected behavior for manganese(II) ($S_{Mn} = {}^5/_2$) and radical ($S_R = {}^1/_2$) Heisenberg ferrimagnetic chains. As the temperature decreases, the χT value increases to about 76 $cm^3\ mol^{-1}\ K$ at 9.1 K and then decreases to 30 $cm^3\ mol^{-1}\ K$ at 2.6 K because of saturation effects. The maximum of χT changes to 199 $cm^3\ mol^{-1}\ K$ at 6.9 K when the magnetic field is reduced to 100 Oe (Figure S4). An estimate of the metal-to-radical magnetic exchange constant ($H = -J\boldsymbol{S}_i\cdot\boldsymbol{S}_i$) was obtained using Seiden's model, considering data above 33 K (see the SI for details), giving $J = -(298 \pm 26)\ cm^{-1}$. This value is within the range found experimentally and by ab initio calculations for other Mn^{II}–NN compounds.[14]

Compound **2** presents a different behavior (Figures S5 and S6), with χT reaching a maximum much higher (750 $cm^3\ mol^{-1}\ K$ for 100 Oe) at 45 K. Below this maximum, χT decreases due to saturation and blocking effects. In contrast with isotropic octahedral manganese(II) complexes, cobalt(II) ions in the same environment have a large magnetic anisotropy. Taking this into account, we used the branch chain model (also considering $H = -J\boldsymbol{S}_i\cdot\boldsymbol{S}_i$) to fit the data for $T \geq 73$ K, obtaining $J = -(162 \pm 13)\ cm^{-1}$ (see the SI for details).

The magnetic correlation length (ξ) and χT (χT is proportional to ξ) increase when the temperature decreases, according to the expression $\chi T = C_{eff}\exp(\Delta_\xi/k_BT)$, where C_{eff} is the effective Curie constant of the chain repeat units and Δ_ξ is the energy required to create a domain wall, which is valid for 1D Ising-like or highly anisotropic Heisenberg systems.[15,16] The exchange interaction within this Ising limit is related to Δ_ξ as $\Delta_\xi = 2|J|S^2$, where S is the ground-state spin quantum number.[8] The domain wall formation energy is $\Delta_\xi/k_B = (379 \pm 12)$ K for **2**, which corresponds to an exchange strength of $|J/k_B| = (190 \pm 6)$ K ($132 \pm 4\ cm^{-1}$) obtained from the slope of a $\ln(\chi T)$ versus $1/T$ plot (Figure S7). There is a ~20% discrepancy between this J value and the one obtained from the branch chain model (233 K), indicating that this system is not within the Ising limit.

The zero-field-cooled (ZFC) magnetic susceptibility of **2** increases strongly just above 10.7 K to a maximum value at 15.7 K (Figure 2). An average blocking temperature was assigned midway between the minimum and maximum susceptibilities, at $T_B \approx 13.2$ K. The field-cooled (FC) susceptibility plateaus over 2.4–10.3 K, slightly increases to a maximum at 12.2 K, and then decreases until it converges with the ZFC curve; the FC and ZFC curves are coincident above 41 K.

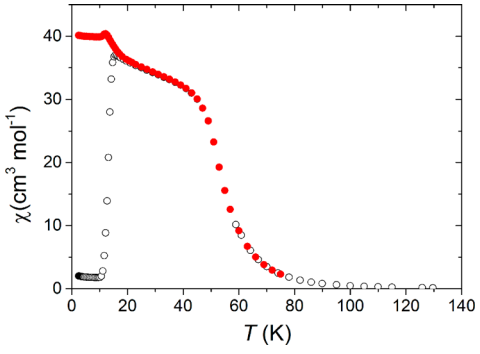

Figure 2. Temperature dependence of ZFC (open circles) and FC (filled circles) magnetic susceptibilities for **2** at 10 Oe.

Magnetization hysteresis curve below the blocking temperature for **2** is shown in Figure 3. At 4.0 K, a large coercive field >49 kOe is observed, while at 8.0 K (see Figure S8), the coercive field is ~30 kOe. The shape of the hysteresis curve suggests the existence of two contributions: one hysteretic with a smooth variation around zero field and a second paramagnetic-like contribution with no hysteresis, responsible for the steep change at low fields.

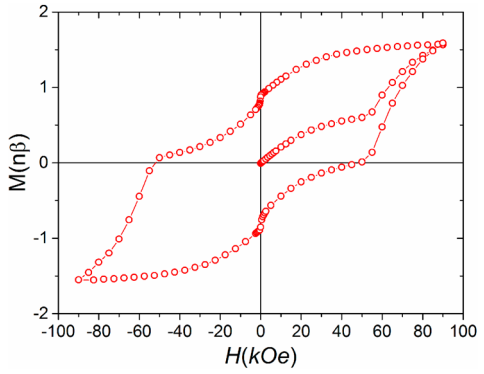

Figure 3. Magnetization hysteresis at 4.0 K for **2**. Note that this is a minor loop and is not fully saturated.

The alternating-current (ac) susceptibility measurements for **2** were performed in zero direct-current (dc) external field (see Figure 4 and the SI). Both the χ' (in-phase) and χ'' (out-of-phase) susceptibility components show frequency dependence consistent with SCM-type behavior. A maximum in χ'' is observed between 20 and 30 K, with a shoulder at higher temperatures (30–45 K) suggesting a broader second relaxation process. This second process can be better discriminated in the isothermal frequency dependence of the susceptibility (Figures S9 and S10). The magnetic relaxation times were obtained from the maxima of χ'' versus T at fixed ac frequencies (20–30 K) and also by fitting χ''

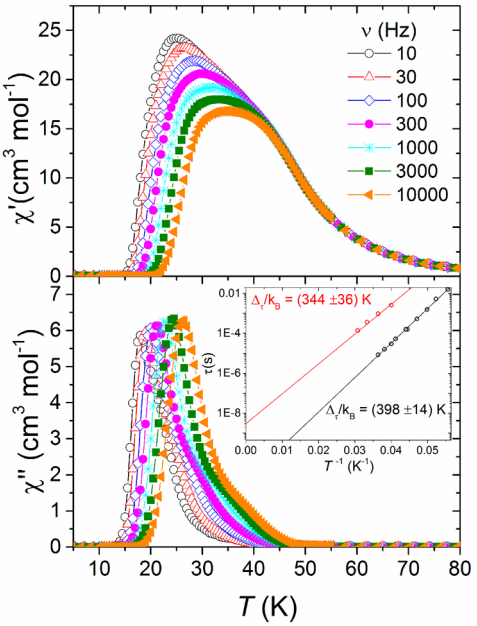

Figure 4. Temperature dependence of χ' (upper) and χ'' (lower) of **2** under zero dc field. Relaxation times versus reciprocal temperature are shown in the inset, where the solid lines represent linear fits to the Arrhenius law.

DOI: 10.1021/acs.inorgchem.5b01431
Inorg. Chem. 2015, 54, 9381–9383

versus ν at fixed temperatures by a sum of two Casimir and Du Pre expressions (see details in the SI). The relaxation times follow an Arrhenius thermal activation behavior $\tau = \tau_0 \exp(\Delta_\tau/k_B T)$ with an activation energy barrier of $\Delta_\tau/k_B = (398 \pm 14)$ K and $\tau_0 = (4 \pm 3) \times 10^{-12}$ s for the lower temperature maxima 20−30 K, while $\Delta_\tau/k_B = (344 \pm 36)$ K and $2 \times 10^{-10} < \tau_0 < 40 \times 10^{-10}$ s for the relaxation process at higher temperatures. Despite the large uncertainty in τ_0 of the latter, one may speculate that their sizes are about a few hundred times longer than the short ones. A standard Cole−Cole analysis of the relaxation data (Figure S11) shows partially overlapped semicircles, confirming two discernible magnetic relaxation processes. At 17.5 K, only the faster relaxation process is observed, with a Cole−Cole parameter $\alpha = 0.19$ indicating a narrow distribution of relaxation times, while at 30.0 K, the slower relaxation process is dominant with $\alpha = 0.45$, showing a broader distribution of relaxation times.

The activation energy barriers associated with the two independent relaxation processes are nearly the same, but the τ_0 values are quite different. Defects have important effects on the relaxation dynamics of SCMs,[7,8,17,18] as shown by studies on SCMs intentionally doped with diamagnetic ions, which showed no dependence of the energy barrier but a clear decrease of τ_0 with increased defect concentration. For nearly defect-free chains, an effectively infinite size regime can be reached, where the relaxation mechanism energy gaps follow the relationship $\Delta_\tau = 2\Delta_\xi + \Delta_A$, where Δ_A is the anisotropy energy. In a finite size regime, the energy gap relationship is $\Delta_\tau = \Delta_\xi + \Delta_A$.[8] In the case of **2**, the experimentally obtained Δ_τ and Δ_ξ show clearly that an effective infinite size regime is not reached ($\Delta_\tau < 2\Delta_\xi$). The presence of two relaxation processes in compound **2** is attributed to the coexistence of a broad distribution of longer chains with a slower relaxation process (longer τ_0) with a dominant narrower distribution of shorter chains having faster relaxation (shorter τ_0).

In existing theories for one-dimensional relaxation models, the relationship between the exchange energy (J) and magnetic anisotropy (D) are important to determine the energy gaps Δ_τ, Δ_ξ, and Δ_A.[7,8] In the Ising limit, the anisotropy is larger than the magnetic exchange energy ($|D/J| > {}^4/_3$), while in the Heisenberg limit the exchange is much larger than the anisotropy ($|J| \gg |D|$).[8] The estimates of the D and J values obtained from the branch chain model give $|D/J| \approx 0.6$, indicating that **2** is neither within the Ising limit nor within the Heisenberg limit. We expect that our results will foster further theoretical studies to determine these relationships.

In conclusion, a SCM with a large coercive field and a high blocking temperature was described. No evidence of three-dimensional magnetic ordering was found in the manganese derivative. For the isostructural cobalt chain, the blocking of the dynamics at temperatures below 13 K would prevent any ordering at lower temperatures. A notable advance here is that NaphNN presents much higher structural stability under ambient conditions than the previous $[Co(hfac)_2(PyrNN)]_n$ chain.

■ ASSOCIATED CONTENT

Supporting Information

The Supporting Information is available free of charge on the ACS Publications website at DOI: 10.1021/acs.inorgchem.5b01431.

Syntheses, thermogravimetry analysis of **2**, and additional magnetic analyses for **1** and **2** (PDF)

Supplementary X-ray crystallographic data in CIF format for **1** and **2** (CIF)

■ AUTHOR INFORMATION

Corresponding Authors

*E-mail: mariavaz@vm.uff.br (M.G.F.V.).

*E-mail: allao.cassaro@iq.ufrj.br (R.A.A.C.).

Author Contributions

All the authors contributed equally to this work.

Notes

The authors declare no competing financial interest.

■ ACKNOWLEDGMENTS

The authors are thankful for the financial support provided by FAPERJ and CNPq (Brazil) and LDRX-UFF (Brazil) for using its laboratory facilities. P.M.L. thanks CNPq (Visiting Researcher; 400808/2012-9).

■ REFERENCES

(1) Gatteschi, D.; Sessoli, R.; Villain, J. *Molecular Nanomagnets*; Oxford University Press: Oxford, U.K., 2006.

(2) Novak, M. A.; Sessoli, R. *Quantum Tunneling of Magnetization—QTM'94*; NATO ASI Series 301; Kluwer Academic Press: Dordrecht, The Netherlands, 1995; pp 171−188.

(3) Ardavan, A.; Rival, O.; Morton, J. J. L.; Blundell, S. J.; Tyryshkin, A. M.; Timco, G. A.; Winpenny, R. E. P. *Phys. Rev. Lett.* **2007**, *98*, 057201.

(4) Mannini, M.; Pineider, F.; Sainctavit, P.; Danieli, C.; Otero, E.; Sciancalepore, C.; Talarico, A. M.; Arrio, M.-A.; Cornia, A.; Gatteschi, D.; Sessoli, R. *Nat. Mater.* **2009**, *8*, 194−197.

(5) Caneschi, A.; Gatteschi, D.; Lalioti, N.; Sangregorio, C.; Sessoli, R.; Venturi, G.; Vindigni, A.; Rettori, A.; Pini, M. G.; Novak, M. A. *Angew. Chem., Int. Ed.* **2001**, *40*, 1760−1763.

(6) Clèrac, R.; Miyasaka, H.; Yamashita, M.; Coulon, C. *J. Am. Chem. Soc.* **2002**, *124*, 12837−12844.

(7) Bogani, L.; Vindigni, A.; Sessoli, R.; Gatteschi, D. *J. Mater. Chem.* **2008**, *18*, 4750−4758.

(8) Coulon, C.; Miyasaka, H.; Clérac, R. *Struct. Bonding (Berlin)* **2006**, *122*, 163−206 Note: Relations were adapted to be in the $H = -JS_i \cdot S_j$ formalism..

(9) Dhers, S.; Feltham, H. L. C.; Brooker, S. *Coord. Chem. Rev.* **2015**, *296*, 24−44.

(10) Heintze, E.; El Hallak, F.; Clauß, C.; Rettori, A.; Pini, M. G.; Totti, F.; Dressel, M.; Bogani, L. *Nat. Mater.* **2013**, *12*, 202−206.

(11) Ishii, N.; Okamura, Y.; Chiba, S.; Nogami, T.; Ishida, T. *J. Am. Chem. Soc.* **2008**, *130*, 24−25.

(12) Vaz, M. G. F.; Cassaro, R. A. A.; Akpinar, H.; Schlueter, J. A.; Santos, S., Jr.; Lahti, P. M.; Novak, M. A. *Chem. - Eur. J.* **2014**, *20*, 5460−5467 Note: The $H = -2JS_i \cdot S_j$ formalism was used..

(13) Vaz, M. G. F.; Allão, R. A.; Akpinar, H.; Schlueter, J. A.; Santos, S., Jr.; Lahti, P. M.; Novak, M. A. *Inorg. Chem.* **2012**, *51*, 3138−3145.

(14) Wei, H.; Wan, F.; Chen, Z. *Sci. China, Ser. B: Chem.* **2005**, *48*, 402−414 and references therein.

(15) Loveluck, J. M.; Lovesey, S. W.; Aubry, S. *J. Phys. C: Solid State Phys.* **1975**, *8*, 3841−3856.

(16) Nakamura, K.; Sasada, T. *J. Phys. C: Solid State Phys.* **1978**, *11*, 331−343.

(17) Bogani, L.; Caneschi, A.; Fedi, M.; Gatteschi, D.; Massi, M.; Novak, M. A.; Pini, M. G.; Rettori, A.; Sessoli, R.; Vindigni, A. *Phys. Rev. Lett.* **2004**, *92*, 207204.

(18) Pini, M. G.; Rettori, A.; Bogani, L.; Lascialfari, A.; Mariani, M.; Caneschi, A.; Sessoli, R. *Phys. Rev. B: Condens. Matter Mater. Phys.* **2011**, *84*, 094444.

■ NOTE ADDED AFTER ASAP PUBLICATION

This paper was posted on September 14, 2015, with incorrect ref citations. The corrected version was reposted on September 17, 2015.

DOI: 10.1021/acs.inorgchem.5b01431
Inorg. Chem. 2015, 54, 9381−9383